# A Deployable Routing System for Nanonetworks

Christos Liaskos*, Angeliki Tsioliaridou*, Sotiris Ioannidis*, Nikolaos Kantartzis† and Andreas Pitsillides‡
*Foundation of Research and Technology - Hellas, GR-70013 Heraklion, Crete, Greece
Emails: {cliaskos, atsiolia, sotiris}@ics.forth.gr
†Aristotle University Thessaloniki, GR-54124, Greece
Email: kant@ece.auth.gr
‡University of Cyprus, 2109 Nicosia, Cyprus
Email: andreas.pitsillides@ucy.ac.cy

***Abstract*—Nanonetworks comprise numerous wireless nodes, assembled at micro-to-nano scale. The unique manufacturing challenges and cost considerations of these networks make for minimal complexity solutions at all network layers. From a networking aspect, packet retransmissions should be kept minimal, while ensuring communication between any two nanonodes. In addition, assigning unique addresses to nanonodes is not straightforward, since it can entail a prohibitively high number of packet exchanges. Thus, efficient data routing is considered an open issue in nanonetworking. The present paper proposes a routing system which can be dynamically deployed within a nanonetwork. Static, dense topologies with numerous, identical nodes are examined. These attributes are especially important in the context of recently proposed applications of nanonetworks. The proposed scheme incurs a trivial setup overhead and requires integer processing capabilities only. Once deployed, it operates efficiently, inducing lower packet retransmission rates than related schemes.** [1]

***Index Terms*—Nanocommunication protocols, wireless networks, nanonetworks, routing.**

## I. Introduction

Advances in nanotechnology have enabled the extension of control and networking to $\mu$m scales. The RFID dust by Hitachi Ltd., for example, comprises nodes that are manufactured at a *total* size of $50\times50\times5$ $\mu$m [1]. Graphene technology is expected to enable even further miniaturization, with interesting applications in a variety of fields. In biomedicine, nano-devices are envisioned to monitor the human body at cellular level, and perform targeted drug delivery [2]. In the materials and environmental monitoring industry, nanonetworking enables the construction of smart, active materials, which enable the real-time monitoring of their internal structural [3], or even the control over their electromagnetic behavior (cf. software-defined materials-SDMs [4]). Such components are expected to extend the reach of programmable (software-defined) networks to the level of material properties. For example, SDMs can be programmed to serve as perfect absorbers or reflectors of electromagnetic energy and light, maximizing the efficiency of renewable energy sources.

Data routing in nanonetworks faces new and unique challenges, stemming from the expectedly "weak" hardware of the nanonodes. This expectation is enforced by several factors [2]. Firstly, the miniature size of the nanonodes naturally translates to assembly restrictions. Secondly, a nanonetwork may contain thousands of nodes, implying a very low-cost nanonode architecture. Despite its low capabilities, the nanonode hardware must face the unique challenges of the THz band, such as high path loss due to molecular absorption, and high ambient noise [5]. These factors imply that nanonetworking is error-prone, and a routing scheme should offer a good degree of path multiplicity. On the other hand, the nanonode power supply is not abundant, and a data routing scheme should keep redundant transmissions low. An additional routing concern is that nanonode addressing is neither unique nor a given [2].

The contribution of this paper is a data routing scheme that respects the nanonetworking considerations in the context of SDMs. The objective of the new scheme is to be dynamically deployable around a selected point, enforcing a system of non-unique addresses as well. Seeking to promote energy efficient networking, the proposed scheme selects few nodes to serve as packet retransmitters first, based on their past reception statistics. Subsequently, a routing process is run by the selected nodes only. Thus, redundant transmissions are limited, while the non-unique addresses ensure a good degree of path multiplicity. The proposed concept also upholds the "weak" hardware assumption. Essentially, it induces very low computational complexity and memory overhead per nanonode, while it assumes integer processing capabilities only.

## II. Related work

Studies on nanonetworking have so far focused on physical-layer specifications (PHY) and medium access control (MAC).

**PHY layer.** Regarding channel models and nanoantennas, studies show that nanonetworking is possible in the THz [6] or in the VHF band [7]. The first case requires graphene antennas [8], whereas the latter is achieved with carbon nanotubes. The modulation and encoding scheme follows the Rate Division Time Spread On-Off Keying (RD TS-OOK) [9]. Nanonodes transmit a logical "1" as a short pulse and a logical "0" as silence. Pulse collisions are possible, unless the interarrival time between logical symbols is randomized prior to each packet transmission. However, this adds complexity due to the need for a handshaking process between nodes. Finally, the nanonode power supply can be based on *energy scavenging* or *wireless power transfer* (WPT). The former

[1]This work was partially supported by the EU Horizon 2020 VirtuWind project (Grant no. 671648).

978-1-4799-6664-6/16/$31.00 ©2016 IEEE

is based on sizable piezoelectric nanogenerators (1000 $\mu m^2$), which can produce enough energy for 1 packet transmission per roughly 10 sec [10]. WPT is more efficient and takes less space ($\mu$m-$n$m) but requires the presence of an external, power-radiating source [11].

**MAC Layer.** Studies have mainly focused on sparse, full-mesh topologies, targeting Body Area Network (BAN) applications [12]. These studies assume hierarchical networks, where a set of sizable, relatively powerful nano-routers control the smaller, cheaper nanonodes. Nonetheless, this approach disrupts the unobtrusive advantage of nanonetworks. Few studies consider ad hoc multi-hop networks of identical nodes, which are the focus of the present work. PHLAME is a distributed MAC protocol running on top of RD TS-OOK, which allows a transmitter and a receiver pair to choose the optimal communication parameters on demand, through a lightweight handshaking process [6]. The Receiver Initiated Harvesting-aware MAC protocol assumes that properly powered nodes advertise their retransmission capability, triggering data dissemination [13]. Both PHLAME and RIH-MAC are built on energy scavenging, thus being applicable to ultra-low network traffic cases. Conceptual similarities also exist among the studied nanonetworks and ad hoc networks-on-chips (NoCs) or macro-scale Wireless Sensor Networks (WSNs) [2]. Nonetheless, NoCs and WSNs assume much more powerful nodes than nanonetworks and very different wireless channel conditions [14]. Therefore, WSN and NoC-oriented solutions are generally not portable to nanonetworks.

Regarding our prior work, the authors presented and evaluated a ray-tracing-based simulation technique for nanonetworks in [15]. A flood-based data dissemination scheme for nanonetworks was proposed in [16]. Given that flood schemes are susceptible to redundant transmissions, [16] introduced a node classification procedure to limit the number of retransmitters. This procedure was then refined to require minimal complexity and integer computations only [17]. A peer-to-peer routing scheme was proposed in [18], which relied on anchor-points and lightweight triangulation to inform the nodes of their location and route packets over short paths. In this case, the location of a node also serves as its address. Concerning *differentiation*, the present study proposes a peer-to-peer scheme that does not require anchors, but instead routes packets on top of a node classification result. Thus, the underlying classification limits the number of possible retransmitters, while the proposed peer-to-peer routing scheme running on top limits packet retransmissions even further.

## III. Assumptions and Prerequisites

The present study assumes nanocommunication at 100 GHz with standard atmospheric conditions. This selection corresponds to a local minimum in terms of path loss due to molecular absorption, while still offering high data rates [19]. The corresponding wavelength is 3 mm, meaning that conventional antennas would be much larger than the intended micro-to-nano scale. Thus, nanonode are assumed to be equipped with graphene antennas. The propagation speed of electromagnetic waves in carbon plasmonic nanoantennas can be orders of magnitude lower than in classical materials, yielding antennas $100-1000$ times smaller than conventional ones for the same wavelength [2]. Finally, the nanonode power supply is based on Wireless Power Transfer [11]. In other words, the power supply of nanonodes is similar to that of existing nano-RFID applications [1]. Thus, the nanonetwork becomes active only in the presence of an external device, which radiates enough energy to cover the needs of each nanonode.

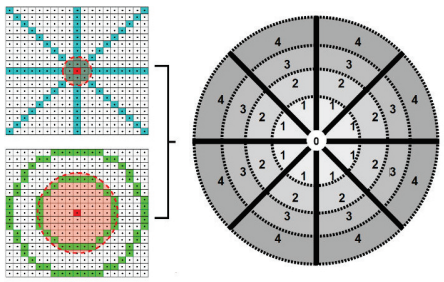

Figure 1. The rationale behind the DEROUS system. DEROUS combines classification results produced by smaller and larger radii to deploy a system of rings and sectors (right inset). Packets can then be routed over the combined system, driven by their distance in hops (N_HOPS) from the beacon O.

In terms of prerequisites, the proposed scheme uses the dynamic infrastructure concept as an underlying sub-process [17]. According to it, an ad hoc network nanonode can deduce, based on its packet reception statistics, whether it should serve as a retransmitter for the other nodes. To this end, a user-selected beacon-node begins to periodically emit packets, which are at first retransmitted blindly by all nodes. During this time, each nanonode simply logs its personal packet receptions statistics in the form of successful/failed packet receptions. Based on these simple integer logs, a node decides if its reception quality is acceptable (i.e., exceeding a given threshold) and accordingly "matures" into "infrastructure" (i.e., blind packet retransmitter) or "user" (non-retransmitting node). We note that this underlying process is self-terminating, lightweight, and virtually instantaneous, given that it can be completed within 3 beacon packet emissions [17]. A key asset is that infrastructure nodes form well-defined and analytically predictable patterns, whose shape depends on the transmission radius of the nodes [16]. Hence, larger radii result into circular patterns around beacon O (Fig. 1 bottom-left inset), while smaller radii yield the manifestation of retransmitters forming radial lines (Fig. 1, top-left inset).

## IV. The Proposed Deployable Routing System (DEROUS)

The general rationale of DEROUS is to combine the radial and circular nanonode classification patterns for the development of an automatically deployable system of segments and sectors, as depicted in Fig. 1. Then, packets can be routed along the circular and radial lines using packet-hop-count information. The goal of DEROUS is to route packets in a peer-to-peer fashion, with low packet collisions and

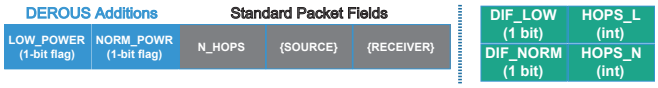


Figure 2. DEROUS requirements in terms of packet header additions (left) and node memory (right).

redundant retransmissions, which are two definitive metrics for the resource-efficiency of a nanonetwork [6], [20].

In terms of general setup, DEROUS assumes *identical* nanonodes, spread over a 2D area following a random or well-defined layout (e.g., a grid). The nanonodes are able to wirelessly transmit packets in two modes: (a) low-power (small radius) and (b) normal power (larger radius). Two phases of operation are defined. A brief deployment phase, and a data routing phase (i.e., standard operation). During deployment, the nanonodes are signaled via proper packet flags to classify themselves as retransmitters/users in low-power, and then (separately) in normal-power transmission mode. These separate classification results are held locally at each node and are properly superimposed during the data routing phase. We note that the assumption of low/normal-power mode is also practical from a different aspect; a low-power transmission mode can be handy when a node is facing a power shortage. DEROUS equips all nodes and packets with the fields shown in Fig. 2 in order to perform the phase signaling and hold the classification results.

The deployment phase of the novel routing system is detailed as follows. Firstly, an external user selects a beacon-node around which he requires the deployment of DEROUS. The beacon begins to periodically emit setup-packets, i.e., with the LOW_POWER flag set to 1 and the N_HOPS field set to 0. The LOW_POWER flag forces all receiving nodes to: (a) enter the low-power transmission mode, (b) retransmit any incoming packet, increasing their N_HOPS value by $+1$, (c) unset their DIF_LOW flags (explained below), and (d) start logging packet reception statistics in order to deduce their retransmitter/user classification according to the related process outlined in Section III. The classification result is held at the DIF_LOW flag, where a value of 1 means that the specific node was classified as a retransmitter (infrastructure) in the low-power transmission mode. In parallel, each node logs its HOPS_L field by setting it equal to the minimum N_HOPS field over the incoming packets, thus denoting the packet hops required to reach this node from the beacon.

Likewise, after the low-power mode terminates, the beacon sets the NORM_POWR flag and repeats the described process in the normal transmission power mode, eventually updating the DIF_NORM and HOPS_N fields. Note that the NORM_POWR and LOW_POWER flags are mutually exclusive, and setting any of them implies that the deployment phase is in progress. In addition, their ordering during the deployment phase is interchangeable. Finally, after both power modes have terminated, the beacon should unset the two DEROUS packet flags, stopping the deployment phase.

Having concluded the deployment phase, DEROUS is able

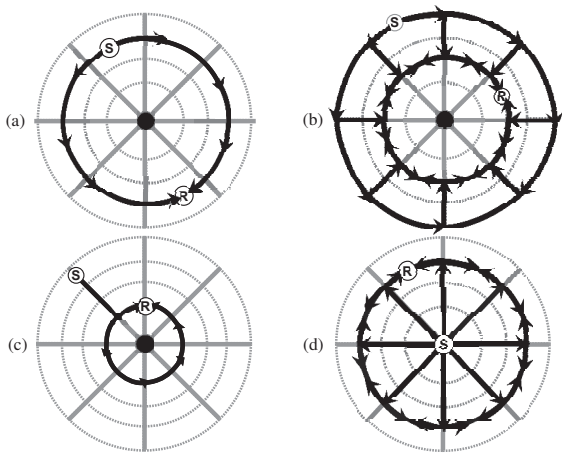


Figure 3. Routing cases of the DEROUS system. The positions of Sender ($S$) and Receiver ($R$) are interchangeable.

to drive a packet $pkt$ from a sender node $S$ to a receiver node $R$ as follows. A node $n$ retransmits an incoming packet if *any* of the following conditions is fulfilled:

$$\begin{gathered}\text{n.HOPS\_N=pkt.S.HOPS\_N } \& \text{ n.DIF\_NORM} \\ \text{n.HOPS\_N=pkt.R.HOPS\_N } \& \text{ n.DIF\_NORM} \\ \text{n.HOPS\_L}\in[\text{pkt.S.HOPS\_L,pkt.R.HOPS\_L}] \ \& \ \text{n.DIF\_LOW}\end{gathered} \tag{1}$$

The first two conditions denote the angular diffusion of packets. According to them, nanonodes placed on a "circle" (i.e., classified as retransmitters during the NORM_POWR mode) should retransmit a packet when the sender or the receiver of the packet are also placed on the same circle. The third condition specifies the radial diffusion of packets. The retransmitters located on radial "lines" (i.e., classified as retransmitters during the LOW_POWER mode) will relay a packet if they are within the two "circles" defined by the sender and the receiver nodes.

We proceed to study the packet routes types produced by DEROUS. For this purpose, we focus on the following general position sets of nodes within the network:

1) Set $C$; nodes on or near (i.e., in range of) a "circle".
2) Set $L$; nodes on or near a radial "line".
3) Set $B$; nodes near the beacon.

Thus, the possible positions of a specific node are defined as:

$$p_i : \left\{ \overset{(i=1)}{C \cap \overline{L} \cap \overline{B}}, \overset{(i=2)}{\overline{C} \cap L \cap \overline{B}}, \overset{(i=3)}{C \cap L \cap \overline{B}}, \overset{(i=4)}{B} \right\}, \tag{2}$$

with $\overline{*}$ representing the complementary set of $*$. In this context, every possible sender-receiver case to be treated by DEROUS is denoted as $p_{ij} = p_i \times p_j$, with $p_{ij} = p_{ji}$ and $i, j = 1 \ldots 4$. Then, the $p_{ij}$ pairs are routed over the paths presented in Fig. 3. Specifically, case $p_{11}$ is routed as depicted in Figs 2(a) and 2(b), depending on whether the sender and receiver are on the same circle. Note that $p_{13}$ and $p_{33}$ are handled in the same manner. Figure 2(c) describes the treatment of $p_{23}$, which also covers $p_{12}$ and $p_{22}$. Finally, cases $p_{i4}$, $\forall i$, are routed as shown in Fig. 2(d).

Notice that DEROUS results into at least two routing paths, for any $p_{ij}$ case. This redundancy is intended as a means to compensate for the challenging nature of nanocommunications [2]. As discussed in Section I, nanonetworking is expected to be error-prone, meaning that routing paths may get frequently segment. DEROUS provides natural path multiplicity to facilitate operation in these expected conditions.

The node identification required/enforced by DEROUS is lightweight and not unique. In essence, a node is identified by the HOPS_L and HOPS_N fields, which determine ring-shaped areas that contain the given node. Specifically, HOPS_N refers to coarse-grained location information, whereas HOPS_L is more fine-grained and reduces retransmissions over the radial paths by adding specificity.

In terms of complexity, DEROUS requires a minimum of 2 and maximum of 7 integer/Boolean comparisons to deduce the outcome of conditions (1). Assuming 8-bit positive integers, the memory footprint of DEROUS is 18 bits per nanonode (cf. right inset of Fig. 2). These requirements are also aligned to the underlying classification process ($O(3)$ integer calculations and 10 bits of node memory respectively, during the deployment phase only [17]).

## V. Simulations

In this Section we evaluate the performance of the proposed DEROUS scheme versus alternative solutions. The simulations were implemented on the AnyLogic platform [21]. The confidence of the presented results is $95\%$.

The comparisons consider related peer-to-peer and flood-based solutions. The first class assumes that a data packet is transferred from one node to another (one-to-one) with a minimum number of intermediate retransmissions. From this class, DEROUS is compared to the COordinate and ROuting system for NAnonetworks (CORONA) [18]. CORONA assumes anchor-nodes and uses triangulation-derived node coordinates as addresses. Regarding the class of flood-based schemes, the comparison considers the probabilistic flood approach (PFLOOD, e.g., [22]) and the Dynamic Infrastructure (DIF) scheme [17]. According to PFLOOD, a node retransmits a received packet randomly, with a given probability. No other criterion is considered. DIF works similarly, but classifies nodes into infrastructure (always retransmit) and users (never retransmit). Flood-based schemes generally convey a packet to all other nodes in the network, including intended and non-intended ones (i.e., one-to-many/all).

**Topology.** The simulations consider 2D topologies, namely a uniform grid and a uniform random layout. The grid layout is studied due to its direct applicability to software-defined metamaterials [4]. The random layout is studied in order to assess the sensitivity of the proposed scheme to layout characteristics. The selected layouts fill a fixed, square area (dimensions $10 \times 10$ mm) with $10,000$ nodes. The nodes are treated as silicon cubes (conductivity 0 S/m, permittivity 2.4 F/m) with a side of 10 $\mu$m. The space among the nodes is filled with air. This topology roughly corresponds to the structure of metamaterials (e.g., [23]). The topology as a whole is intended to approximate a software-defined metamaterial application.

Table I
Simulation Parameters

| Parameter | Value |
|---|---|
| **Communication & Power Parameters** | |
| Frequency | 100 GHz |
| Normal Tx Power ($P_{TX}$) | 2 dBnW |
| Low Tx Power ($P_o$) | Grid$\rightarrow -13$ dBnW |
| | Random$\rightarrow -7$ dBnW |
| Noise Level | 0dBnW |
| $\text{SINR}_{thresh}$ | $-10$ dB |
| Guard Interval | 0.1 nsec |
| Packet Duration | 10nsec |
| Power Supply | Wireless Power Transfer [11] |
| **Path Attenuation Parameters** | |
| Absorption Coefficient $K$ | 0.52 dB/Km (default) |
| Shadow Fading Coefficient $X$ | 2 dB (default) |
| **Simulation Run Parameters** | |
| Simulation Duration (in attempted node-pair comm.) | 100 |
| Beacon Position | Center-most node |

**Channel Model.** The simulations use a full-3D ray tracing approach to deduce the propagation paths, their timing and attenuation [15]. Diffractions, reflections and refractions are considered. All nodes are equipped with isotropic antennas. In order to keep the ray-tracing process computationally tractable, we only consider rays within a radius around a transmitting node. This connectivity *radius* ($\approx 0.95$ mm) is defined by the Tx Power, the Noise Level, the $\text{SINR}_{thresh}$ and the path loss, $L$:

$$\frac{P_{\text{TX}}}{\text{Noise} \cdot L(radius)} > \text{SINR}_{thresh} \quad (3)$$

Molecular absorption due to the air (absorption coefficient $K$ [24]) and shadow fading ($X$ coefficient in dB [25]) are taken into account. The default value of $K$ is set to $0.52$ dB/Km, which corresponds to absorption due to standard atmospheric gasses at 100 GHz (see [19, p. 3 and p. 16]). This value corresponds to normal humidity (7.5 gr/m$^3$). The shadow fading coefficient is modeled as a Gaussian random variable with standard deviation $X$ in dB, varying the path loss as $L_{\text{dB}}(radius) + X$ [25]. To the best of the authors' knowledge, there are presently no real-world measurements of $X$ that pertain specifically to nanonetworking environments. On one hand, higher-frequency studies (300 GHz) approximate $X$ at 1.905 dB for cm distances [25]. On the other hand, studies at 94 GHz-but at $\sim$m distances-place $X$ within the range $0.6 - 5$ dB, with the value 1.8 being representative for most studied cases [26]. In light of these studies, and in absence of nanonetworking-specific measurements, we will use a default value of $X = 2$ dB.

**Simulation parameters and setup.** The communication-related parameters are summarized in Table I. We employ the SINR approach (Signal to Interference plus Noise Ratio) to simulate the packet reception process [27] The selected *Normal Tx Power* (Table I) corresponds via inequality (3) to a maximum radius of 0.95 mm. The *Low Tx Power*

of $-13$ dBnW (applicable to DEROUS only), is used in the grid layout and is carefully selected to correspond to a radius that includes the eight immediate neighbors of a given node. The *Low Tx Power* used in the random layout is raised in order to avoid creating disconnected topologies due to the randomization on the nodes' positions, thus facilitating the simulations. The remaining simulation parameters are set *by expectation* [10], and their values need only hold *by ratio*, as expressed by equation (3). The noise level in nanonetworks is expected to be high compared to their Tx Power, due to the presence of molecular noise apart from the common thermal noise [24]. As a result, nanonetworks will operate under very low SINR thresholds [28]. Nonetheless, theoretical lower bounds exist for this parameter. We therefore choose indicatively the mean lower bound for the simplest kind of receiver, i.e., $-10$ dB [29]. A Guard Interval of $0.1$ nsec is assumed, meaning that multiple receptions of the same packet arriving within this interval add up to the power of the useful signal. This choice expresses the expectation that the weak nanonode hardware may be sensitive even to mild interference.

We assume that the node that is nearest to the center of the topology is the *beacon* around which DEROUS is deployed. We allow for a 3 sec warm-up for all compared schemes. Then, with an inter-arrival time of 1 sec, we randomly select a sender and a receiver among the nodes. The sender sends a single packet, which is transferred to the receiver in a manner defined by each compared scheme. We repeat this process for $100$ random pairs and we log:

- The successful original-sender-to-final-receiver node packet exchange ratio (i.e., how many out of the $100$ random sender-receiver pairs communicated successfully).
- The number of intermediate retransmitting nodes involved in each of the $100$ packet exchanges, forming a probability distribution function (PDF).
- The global (i.e., network-wide) aggregate: i) number of packets sent from all nodes (*Sent Rate*), ii) number of packets successfully received by all nodes (*Recv. Rate*), iii) number of erroneous packet receptions due to interference (*Interf. Rate*). These metrics are defined as the aggregates over all nodes and over all $100$ exchanges, divided by the duration of the simulation (i.e., the time for $100$ exchanges).

**Results.** Figures 4 and 5 present the results pertaining to the grid layout. The PDF of nodes involved per transmission pair is given in Fig. 4. As expected, the PFLOOD approach involves every single of the $10,000$ nodes in the network, for each transmission pair, when the flood probability is $1.0$ (PFLOOD-1.0). This number drops proportionally to the flood probability, when the latter is decreased to $p = 0.8, 0.6, 0.4$ respectively. Notice that the respective PDFs are narrow peaks around the means defined by $p \times 10,000$. We remark that $p$ is a parameter that requires manual, precise tuning, which may not be viable for nanonetworks, since adapting it adds considerable complexity and overhead [16]. For example, Fig. 5 demonstrates that even wild variations of $p$ may offer small

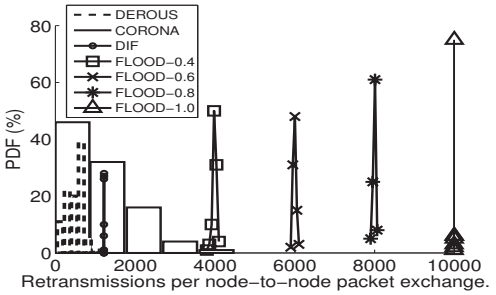


Figure 4. Probability distribution function (PDF) of nodes involved in the transmission of a packet from a random source to a random destination. A grid topology is used. DEROUS offers the best performance.

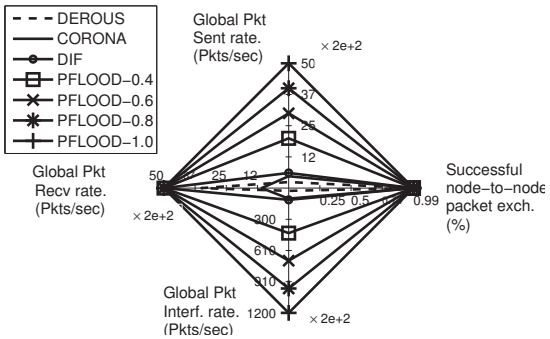


Figure 5. Radar plot for the setup of Fig. 4, presenting the successful packet transmission ratio, as well as the global packet send/receive/loss rate.

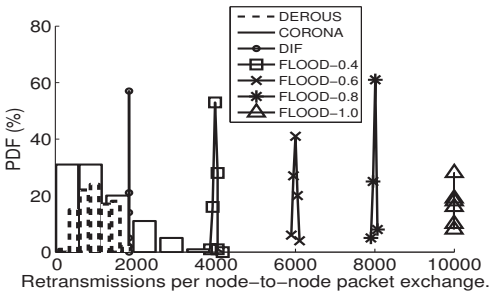


Figure 6. PDF of nodes involved in the transmission of a packet from a random source to a random destination, assuming a random topology.

performance advantage. All compared PFLOOD variations achieve the same packet exchange and global packet reception rates as DIF and DEROUS, while incurring the highest global packet transmission and packet loss rates.

The DIF scheme performs much better than PFLOOD in any case, without requiring any tuning. However, in Fig. 4 we notice that the corresponding PDF is a very narrow peak around an average of $\sim 1200$ retransmissions. This number is approximately equal to the number of nodes elected to serve as retransmitters by the DIF scheme. In other words, for each random sender-receiver pair, the complete Dynamic Infrastructure participates to the packet transmission process. DIF also surpasses PFLOOD in Fig. 5.

CORONA employs a variable number of retransmitters per

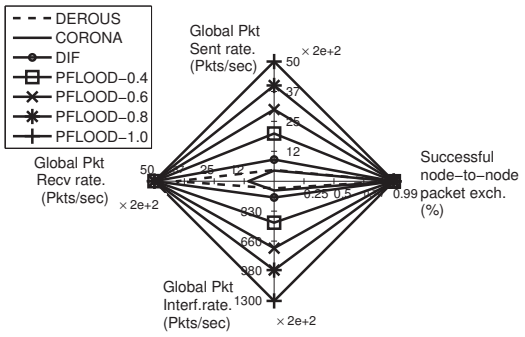


Figure 7. Radar plot for the setup of Fig. 6, presenting the successful packet transmission ratio, as well as the global packet send/receive/loss rate.

communicating pair (Fig. 4). It performs better than PFLOOD in any case, similarly or better than DIF and worse than DEROUS. Being a peer-to-peer scheme, CORONA uses just a few of the nodes within the network to perform the routing. Thus, the low global reception rate in Fig. 5 is natural and does not constitute a sign of impaired performance. Nonetheless, DIF also selects very few nodes to serve as retransmitters, thus closing in on CORONA, despite its flood-based nature.

DEROUS applies peer-to-peer routing over the few selected retransmitters, naturally outperforming PFLOOD, DIF and CORONA. In Fig. 4 we observe that the PDF of DEROUS is not a narrow peak, meaning that the number of retransmitters participating to a packet exchange varies considerably. This is expected, given that the packets now travel over selected circular and radial paths, as described in Section IV. In essence, the performance of DIF is a worst-case, low-probability scenario for DEROUS. On average, DEROUS yields half of the retransmissions required by DIF or CORONA, while it exhibits the best performance in Fig. 5 as well.

Finally, the ranking of the compared schemes is retained in the random layout, presented in Fig. 6 and 7. In such layouts, the dynamic infrastructure patterns are no longer clear, straight lines and circles, but exhibit a degree of fuzziness, generally involving more retransmitters [16]. Thus, the corresponding PDF in Fig. 6 exhibits increased mean value and variance compared to Fig. 4. Despite this behavior, DEROUS continues to function as expected, showing that well-arranged topologies are not an operational requirement.

## VI. Conclusion

The present study introduced a deployable routing system (DEROUS) for ad hoc nanonetworks, targeting applications in software-defined materials (SDMs) [4]. DEROUS dynamically forms circular and radial packet routing paths around a given beacon point. These paths were shown to efficiently serve peer-to-peer communication needs, while reducing considerably the number of required packet retransmissions. Incurring a negligible overhead on the nanonodes, DEROUS constitutes an enabling factor for SDMs, allowing for highly anticipated, future nanonetworking applications in industrial materials and highly efficient renewable energy sources.

## References


[1] T. Hornyak, "RFID Powder," *Scientific American*, vol. 298, no. 2, pp. 68–71, 2008.

[2] I. Akyildiz and J. Jornet, "The Internet of nano-things," *IEEE Wireless Communications*, vol. 17, no. 6, pp. 58–63, 2010.

[3] International Atomic Energy Agency, "Characterization and Testing of Materials for Nuclear Reactors," in *Proc. of the IAEA technical meeting 2006*, vol. IAEA-TECDOC-1545.

[4] C. Liaskos *et al.*, "Building Software Defined Metamaterials with Nanonetworks," *IEEE Circuits and Systems Magazine*, 2015.

[5] J. Jornet and I. Akyildiz, "Channel capacity of electromagnetic nanonetworks in the terahertz band," in *Proc. of IEEE ICC'2010*.

[6] J. Jornet *et al.*, "PHLAME: A Physical Layer Aware MAC protocol for Electromagnetic nanonetworks in the Terahertz Band," *Nano Communication Networks*, vol. 3, no. 1, pp. 74–81, 2012.

[7] J. Lehtomaki, I. Akyildiz *et al.*, "On the Nanoscale Electromechanical Wireless Communication in the VHF Band," *IEEE Transactions on Communications*, vol. 63, no. 1, pp. 311–323, 2015.

[8] Q. Liu, P. He, K. Yang, and S. Leng, "Inter-symbol interference analysis of synaptic channel in molecular communications," in *Proc. of IEEE ICC'2014*, pp. 4424–4429.

[9] J. Jornet and I. Akyildiz, "Low-weight channel coding for interference mitigation in electromagnetic nanonetworks in the terahertz band," in *Proc. of IEEE ICC'2011*.

[10] J. Jornet, "A joint energy harvesting and consumption model for self-powered nano-devices in nanonetworks," in *Proc. of IEEE ICC'2012*.

[11] A. Lalas *et al.*, "Powering Nanonetworks by Exploiting Metamaterial-Inspired Wireless Energy Transfer," in *Proc. of IEEE NANO'15*.

[12] G. Piro *et al.*, "On the design of an energy-harvesting protocol stack for Body Area Nano-NETworks," *Nano Communication Networks*, vol. 6, no. 2, pp. 74–84, 2015.

[13] M. Shahram and C. Michele, "RIH-MAC: Receiver-Initiated Harvesting-aware MAC for NanoNetworks," in *Proc. of ACM NANOCOM'14*. ACM, pp. 180–188.

[14] M. Younis *et al.*, "Topology management techniques for tolerating node failures in wireless sensor networks: A survey," *Computer Networks*, vol. 58, pp. 254–283, 2014.

[15] K. Kantelis *et al.*, "On the Use of FDTD and Ray-Tracing Schemes in the Nanonetwork Environment," *IEEE Communications Letters*, vol. 18, no. 10, pp. 1823–1826, 2014.

[16] C. Liaskos and A. Tsioliaridou, "A Promise of Realizable, Ultra-Scalable Communications at nano-Scale," *IEEE Transactions on Computers*, vol. 64, no. 5, pp. 1282–1295, 2015.

[17] A. Tsioliaridou *et al.*, "Lightweight, Self-tuning Data Dissemination for Dense Nanonetworks," *Elsevier Nano Comm. Netw., in press*, 2015.

[18] ——, "CORONA: A Coordinate and Routing system for Nanonetworks," in *Proc. of ACM NANOCOM'15*, 2015.

[19] ITU-R, "Rec. P.676-7: Attenuation by atmospheric gases," Feb. 2007.

[20] P. Wang *et al.*, "Energy and spectrum-aware MAC protocol for perpetual wireless nanosensor networks in the Terahertz Band," *Ad Hoc Networks*, vol. 11, no. 8, pp. 2541–2555, 2013.

[21] X. Technologies, "The AnyLogic Simulator," 2013. [Online]. Available: http://www.xjtek.com/anylogic/

[22] T. Zhu *et al.*, "Achieving Efficient Flooding by Utilizing Link Correlation in Wireless Sensor Networks," *IEEE/ACM Transactions on Networking*, vol. 21, no. 1, pp. 121–134, 2013.

[23] T. Bckmann *et al.*, "Tailored 3D mechanical metamaterials made by dip-in direct-laser-writing optical lithography," *Advanced materials (Deerfield Beach, Fla.)*, vol. 24, no. 20, pp. 2710–2714, 2012.

[24] J. Jornet and I. Akyildiz, "Channel Modeling and Capacity Analysis for Electromagnetic Wireless Nanonetworks in the THz Band," *IEEE Trans. on Wireless Comm.*, vol. 10, no. 10, pp. 3211–3221, 2011.

[25] S. Kim and A. Zajic, "A path loss model for 300-GHz wireless channels," in *Proc. of IEEE ISAP'14*, pp. 1175–1176.

[26] A. Kajiwara, "Indoor propagation measurements at 94 GHz," in *Ptoc of IEEE PIMRC'95*, pp. 1026–1030.

[27] A. Iyer *et al.*, "What is the right model for wireless channel interference?" *IEEE Trans. on Wir. Comm.*, vol. 8, no. 5, pp. 2662–71, 2009.

[28] P. Boronin *et al.*, "Capacity and throughput analysis of nanoscale machine communication through transparency windows in the terahertz band," *Nano Communication Networks*, vol. 5, no. 3, pp. 72–82, 2014.

[29] R. Tandra and A. Sahai, "Fundamental limits on detection in low SNR under noise uncertainty," in *Proc. of the IWCMC'05*, pp. 464–469.